Activation and Inhibition of Pyruvate Carboxylase from *Rhizobium etli*

Tonya N. Zeczycki,[†] Ann L. Menefee,[‡] Sarawut Jitrapakdee,[§] John C. Wallace,[∥] Paul V. Attwood,[⊥] Martin St. Maurice,[‡] and W. Wallace Cleland*,[†]

[†]Institute for Enzyme Research and Department of Biochemistry, University of Wisconsin, Madison, Wisconsin 53726, United States

[‡]Department of Biological Sciences, Marquette University, Milwaukee, Wisconsin 53201, United States

[§]Department of Biochemistry, Faculty of Science, Mahidol University, Bangkok 10400, Thailand

[∥]School of Molecular and Biomedical Science, University of Adelaide, Adelaide S.A., 5005, Australia

[⊥]School of Biomedical, Biomolecular and Chemical Sciences, University of Western Australia, Crawley WA, 6009 Australia

S *Supporting Information*

ABSTRACT: While crystallographic structures of the *R. etli* pyruvate carboxylase (PC) holoenzyme revealed the location and probable positioning of the essential activator, Mg^{2+}, and nonessential activator, acetyl-CoA, an understanding of how they affect catalysis remains unclear. The current steady-state kinetic investigation indicates that both acetyl-CoA and Mg^{2+} assist in coupling the MgATP-dependent carboxylation of biotin in the biotin carboxylase (BC) domain with pyruvate carboxylation in the carboxyl transferase (CT) domain. Initial

velocity plots of free Mg^{2+} vs pyruvate were nonlinear at low concentrations of Mg^{2+} and a nearly complete loss of coupling between the BC and CT domain reactions was observed in the absence of acetyl-CoA. Increasing concentrations of free Mg^{2+} also resulted in a decrease in the K_a for acetyl-CoA. Acetyl phosphate was determined to be a suitable phosphoryl donor for the catalytic phosphorylation of MgADP, while phosphonoacetate inhibited both the phosphorylation of MgADP by carbamoyl phosphate ($K_i = 0.026$ mM) and pyruvate carboxylation ($K_i = 2.5$ mM). In conjunction with crystal structures of T882A *R. etli* PC mutant cocrystallized with phosphonoacetate and MgADP, computational docking studies suggest that phosphonoacetate could coordinate to one of two Mg^{2+} metal centers in the BC domain active site. Based on the pH profiles, inhibition studies, and initial velocity patterns, possible mechanisms for the activation, regulation, and coordination of catalysis between the two spatially distinct active sites in pyruvate carboxylase from *R. etli* by acetyl-CoA and Mg^{2+} are described.
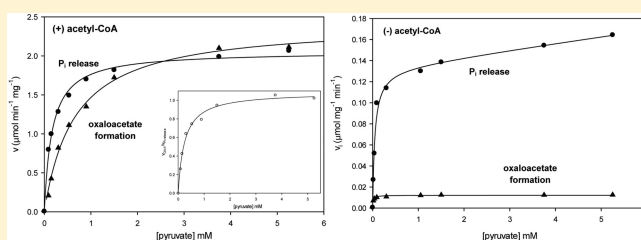
**P**yruvate carboxylase (PC; E.C 6.4.1.1) is an essential regulatory, anaplerotic enzyme which catalyzes the MgATP-dependent carboxylation of pyruvate by HCO_3^- to form oxaloacetate, MgADP and P_i.[1] The oxaloacetate formed is either fed directly into the citric acid cycle where the intermediates are removed for various metabolic pathways including gluconeogenesis in liver,[1] *de novo* fatty acid biosynthesis in adipose tissue, synthesis of neurotransmitters in the brain, and glucose-induced insulin secretion in pancreatic islets.[2] The significance of PC activity in intermediary metabolism and the importance of the regulation of this activity by allosteric activators, such as acetyl-CoA, and inhibitors, including L-aspartate, have been shown in recent studies where increased PC activity is linked to the pathogenesis of a variety of diseases. For example, a positive correlation between aberrant PC activity and the proliferation of tumor cells has been established through the ^{13}C-isotopologue analysis of metabolites in cancer patients,[3] while the enhanced PC gluconeogenic activity detected in the liver of type 2 diabetic patients is partly responsible for the overabundant production of glucose in the liver.[4] An increase in the transcription levels and the activity of PC in both *Listeria*

monocytogenes[5] and *Staphylococcus aureus*[6] have been correlated with intensified bacterial virulence.

The three individual functional domains of α_4 pyruvate carboxylases, including PC from *R. etli* (*Re*PC), are arranged on a single polypeptide chain,[1] with the PC-catalyzed carboxylation of pyruvate occurring in two steps at spatially distinct active sites (Scheme 1). The concurrent deprotonation of
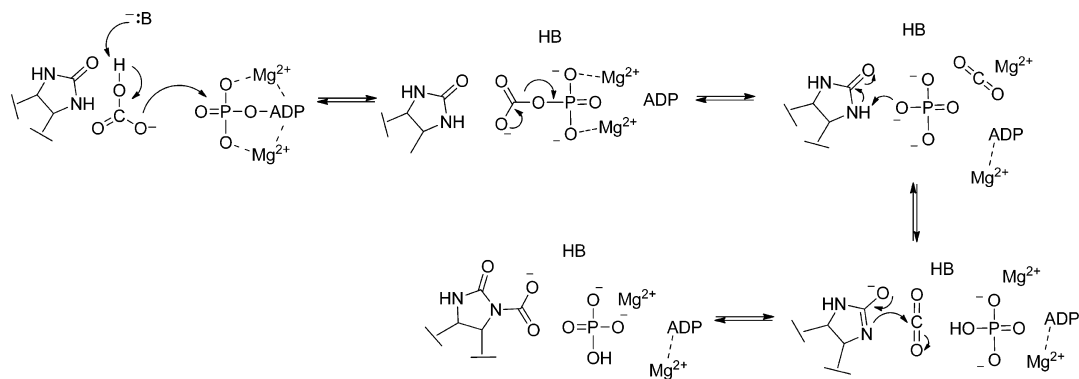
Scheme 1. Overall Reaction Catalyzed by *Re*PC
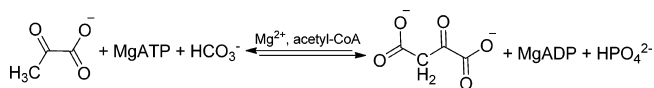
HCO_3^- and cleavage of MgATP in the biotin carboxylase (BC) domain results in the formation of a carboxy phosphate intermediate, which reversibly decomposes into CO_2 and

Scheme 2. A Generalized Mechanism of the MgATP-Dependent Carboxylation of Biotin in the BC Domain[a]

[a]B is the general base required to deprotonate HCO_3^-.

PO_4^{3-}. The biotin carboxyl carrier protein (BCCP) domain carries the biotin cofactor, which is covalently attached to Lys1119,[a] between the BC and carboxyl transferase (CT) domains. PO_4^{3-} migrates in the BC domain active site to position itself near the tethered biotin binding pocket (Scheme 2). Acting as an active site base, PO_4^{3-} deprotonates biotin at the N_1-position to form the biotin enolate which then reacts with CO_2 to produce carboxybiotin. Further details of the proposed catalytic mechanism of the BC domain are presented in the accompanying article.[7] The tethered carboxybiotin is then translocated to the CT domain active site on a neighboring polypeptide chain, via the movement of the BCCP domain,[8] releasing MgADP and P_i from the BC domain active site. Enolization of pyruvate in the CT domain, promoted by coordination to the Lewis acid metal center in the active site, and proton transfer to the biotin enolate are facilitated by a strictly conserved Thr residue.[9] CO_2 then reacts with the nucleophilic enol−pyruvate intermediate, resulting in the formation of oxaloacetate.

While the chemical and kinetic mechanisms of pyruvate carboxylation catalyzed by α_4 PCs from different organisms are expected to be similar, the regulation of the activity and sensitivity to inhibitors and activators, including acetyl-CoA and divalent cations, can vary depending on the physiological differences in the metabolism of the organisms from which the enzyme originates.[10] Additionally, metabolic differences between *R. etli*, a strict aerobe,[11] and *S. aureus*, a facultative anaerobe,[12] may, in part, result in the substantial quaternary structural differences observed in the α_4 PC holoenzymes.[8,13,14] The inherent asymmetry of the *Re*PC tetramer observed when ethyl-CoA is bound in the allosteric site[8] or when cocrystallized with either acetyl-CoA or the allosteric inhibitor, L-aspartate,[13] alludes to the possible differential activation and regulation of *Re*PC by acetyl-CoA compared to *Sa*PC, which is symmetric even in the presence of acetyl-CoA.[14] Interestingly, only two of the four allosteric active sites are occupied by ethyl-CoA in the *R. etli* holoenzyme structures while all four allosteric sites in *Sa*PC contain the activator.

The structural differences between *Re*PC and *Sa*PC prompted, in part, the characterization of the acetyl-CoA and Mg^{2+} activation of *Re*PC presented here. The current study examined the effects of acetyl-CoA and Mg^{2+} on the activities of the full forward and reverse reaction as well as the partial reactions occurring at each active site. Initial velocity studies show that both Mg^{2+} and acetyl-CoA aid in coordinating the chemistry occurring in each of the domains such that MgATP

cleavage and biotin carboxylation in the BC domain are coupled to pyruvate carboxylation in the CT domain at saturating concentrations of pyruvate, Mg^{2+}, and acetyl-CoA. Acetyl phosphate was found to be a suitable phosphoryl donor in the *Re*PC-catalyzed phosphorylation of MgADP. pH profiles and inhibition studies of the pyruvate carboxylation and MgADP phosphorylation reactions with phosphonoacetate give new insight into the reactions in the BC domain of wild-type *Re*PC. These studies along with the new structural description of *Re*PC containing BCCP−biotin in the BC domain[13] and the rigorous site-directed mutagenesis study focusing on the BC domain active site of *Re*PC[7] presented in the accompanying articles allow for a more comprehensive picture of the complex regulation and activation of pyruvate carboxylation catalyzed by *Re*PC.

■ MATERIALS AND METHODS

Materials. IPTG, biotin, NADP, NADH, ampicillin, and chloramphenicol were purchased from Research Products International Corp. (RPI). Ni^{2+}-Profinity IMAC resin was obtained from Bio-Rad. The Pierce BCA Assay kit was purchased from Thermo Scientific, and the EnzChek Phosphate Assay kit was purchased from Invitrogen. All other materials were obtained from Sigma-Aldrich and of the highest purity available.

Methods. *Mutagenesis, Overexpression, and Purification of Protein.* Preparation and purification of the wild-type and T882A and K1119Q *Re*PC mutants were performed as previously described.[9] The proteins were purified using Ni^{2+}-affinity chromatography, concentrated to approximately 2−6 mg/mL and used without further purification. The nearly complete (>98%) biotinylation of the wild-type and the T882A *Re*PC mutant and lack of biotinylation in the K1119Q mutant were confirmed via an avidin binding gel-shift assay.[9]

Enzymatic Assays. The coupled assay systems used to determine the initial rates of the overall forward and reverse reactions as well as the partial reactions of the individual domains are similar to those described previously[9] and further detailed in the accompanying article.[7] Specific reaction conditions are discussed below. In most cases, the mixed buffer system (50 mM Bis-Tris, 25 mM tricine, and 25 mM glycine) was used as a replacement for the 100 mM tricine buffer used previously.

Pyruvate Carboxylation Activity and Determination of Initial Velocity Patterns. Pyruvate carboxylation activity was measured using the malate dehydrogenase coupled assay in reaction volumes of 1 mL (25 °C, pH 7.5). Concentrations of

MgATP stock solutions were determined via end-point analysis using the hexokinase/glucose-6-phosphate coupled assay system, pyruvate was determined using lactate dehydrogenase, and HCO_3^- was determined using phosphoenolpyruvate carboxylase/malate dehydrogenase. Initial velocity patterns were determined by measuring the initial rates of the overall reaction at various concentrations of one substrate or pseudosubstrate (Mg^{2+}, MgATP, acetyl-CoA, or pyruvate) at fixed concentrations of a second substrate. All other reaction components were held constant at saturating concentrations. For the determination of the patterns between free Mg^{2+} and MgATP, reactions contained 12 mM pyruvate, 15 mM HCO_3^-, $MgCl_2$ (1.09−7.44 mM), MgATP (0.058−3.4 mM), 0.25 mM acetyl-CoA, 0.24 mM NADH, and malate dehydrogenase (10 U). For reactions where pyruvate (0.18−13 mM) was varied at fixed concentrations of free Mg^{2+} (1.0−7.8 mM), 25 mM HCO_3^-, 2.5 mM MgATP, and 0.25 mM acetyl-CoA were held constant. Similarly, when acetyl-CoA (0.0−0.3 mM) was varied at fixed Mg^{2+} (0.5−3.0 mM), 12 mM pyruvate, 15 mM HCO_3^-, and 2.5 mM MgATP were held constant.

To accurately determine the K_m for HCO_3^- in the pyruvate carboxylation reaction, buffers and stock solutions of the reaction cocktails were sparged with CO_2-free N_2 at pH 7.5 overnight to remove any endogenous CO_2. To prepare the HCO_3^- stock solutions, NaHCO3 was added to round-bottom flasks equipped with a stopcock arm and rubber septum. The flasks were sealed and flushed with CO_2-free N_2 for 1 h prior to the addition of distilled water via syringe. 1.5 mL cuvettes were stoppered with rubber septa and flushed with N_2 for 5−10 min prior to the addition of the sparged reaction components. Control reactions indicated that the small amount of CO_2 introduced into the system from the enzyme solutions had no effect on the rates. The k_{cat} and k_{cat}/K_m for HCO_3^- were determined at pH 7.5 in 1 mL reaction volumes containing HCO_3^- (0.35−20 mM), 12 mM pyruvate, 5.0 mM $MgCl_2$, 3.0 mM MgATP, 0.25 mM acetyl-CoA, 0.24 mM NADH, and malate dehydrogenase (10 U). The dependence of k_{cat} and $k_{cat}/K_{m,MgADP}$ on pH in the full forward reaction was determined in assays similar to those above where MgATP was the variable substrate (0.05−3.2 mM) in 1 mL total reaction volumes. The mixed buffer system used for all the kinetic studies (50 mM Bis-Tris, 25 mM tricine, 25 mM glycine) effectively buffered the reactions throughout the range of pH values examined while maintaining a constant ionic strength.[15] All other substrates and activators were held at fixed, saturating concentrations and k_{cat} and k_{cat}/K_m values were determined at each pH (6.7−8.6). 25 mM of HCO_3^- was added to the reactions. While the actual concentration of HCO_3^- in the reaction mixtures will vary with pH, the amount of HCO_3^- present is still sufficient to saturate the enzyme. The initial rates of the wild-type-catalyzed carboxylation of pyruvate were also determined in the presence of fixed concentrations of phosphonoacetate (0−6.0 mM) and varying concentrations of MgATP (0.16−2.0 mM). All reactions (25 °C, 1 mL) were initiated with the addition of wild-type RePC (5−25 µg) and contained 50 mM Bis-Tris, 25 mM tricine, 25 mM glycine (pH 7.5), 25 mM HCO_3^-, 12 mM pyruvate, 5.0 mM $MgCl_2$, 0.25 mM acetyl-CoA, 0.24 mM NADH, and malate dehydrogenase (10 U).

Activities of the Full Reverse Reaction. The initial rates of the full reverse reaction were determined using the hexokinase/ glucose-6-phosphate dehydrogenase coupled assay system. The k_{cat} and k_{cat}/K_m were determined by varying MgADP (0.05−1.0 mM). The 3 mL reactions (pH 7.5, 25 °C) contained 7.0 mM

$MgCl_2$, 2.5 mM phosphate, 1.0 mM oxaloacetate, 0.3 mM glucose, 0.25 mM acetyl-CoA, 0.24 mM $NADP^+$, glucose-6-phosphate dehydrogenase (5 U), and hexokinase (1 U). Specific activities were also determined in the presence and absence of acetyl-CoA, in triplicate, and the standard errors reported are the standard deviations of the three runs. The dependence of k_{cat} and $k_{cat}/K_{m,MgADP}$ for the full reverse reaction on pH was also determined under analogous conditions at varying pH (6.0−8.5).

HCO_3^--Dependent ATPase Activity in the Absence of Pyruvate. The EnzChek Phosphate assay system (Invitrogen) was used to determine the initial rates of P_i release. Initial rates were determined by monitoring the corresponding increase in absorbance at 360 nm due to the formation of 2-amino-6-mercapto-7-methylpurine from the PNP-catalyzed phosphorylation of MESG by P_i. The extinction coefficient for 2-amino-6-mercapto-7-methylpurine at 360 nm was determined to be 6300 cm^{-1} M^{-1} under conditions similar to those used for the RePC catalyzed reaction (50 mM Bis-Tris, 25 mM tricine, 25 mM glycine, 20 mM HCO_3^-, pH 7.5, 25 °C) and was used for all subsequent calculations. The k_{cat} and $k_{cat}/K_{m,MgATP}$ for the wild-type RePC-catalyzed MgATP-cleavage reaction was determined at 25 °C in 1 mL total reaction volumes. Reactions contained 20 mM HCO_3^-, 5.0 mM $MgCl_2$, MgATP (2.6−450 µM), 0.25 mM acetyl-CoA (unless otherwise indicated), 0.2 mM MESG, and PNP (3 U).

Oxamate-Induced Decarboxylation of Oxaloacetate. The specific activities of oxaloacetate decarboxylation in the presence of oxamate were monitored in the presence and absence of acetyl-CoA using the lactate dehydrogenase coupled assay. The 3 mL reactions contained 50 mM Bis-tris, 25 mM tricine, 25 mM glycine (pH 7.5, 25 °C), 1 mM oxamate, 0.95 mM oxaloacetate, 0.25 mM acetyl-CoA (unless otherwise indicated), 0.24 mM NADH, and lactate dehydrogenase (10 U). Specific activities were determined in triplicate, and standard errors reported are the standard deviations from the three trials.

Phosphorylation of MgADP Using Acetyl Phosphate or Carbamoyl Phosphate as a Phosphoryl Donor. Carbamoyl-phosphate and acetyl phosphate solutions were made just prior to use and kept on ice for the duration of the assay experiments. In order to remove contaminating nucleotides, a 0.2 M acetyl phosphate solution (85% purity) was acidified (pH 2.0) and stirred with activated charcoal for 30 min. After filtering, the solution was lyophilized and used for all subsequent experiments. The phosphorylating ability of the wild-type and the RePC mutants were determined by measuring the amount of MgATP production using the hexokinase/glucose-6-phosphate dehydrogenase coupled assay at various concentrations of either carbamoyl phosphate (1.0−20 mM) or acetyl phosphate (0.1−20 mM) and in the presence or absence of 10 mM free biotin. All assays were performed at 25 °C and a total reaction volume of 1 mL. Reactions contained 3.5 mM MgADP, 7.5 mM $MgCl_2$, 0.25 mM acetyl-CoA (unless otherwise indicated), 0.4 mM glucose, 0.36 mM NADP, glucose-6-phosphate dehydrogenase (5 U), and hexokinase (1U). The effect of free Mg^{2+} on the initial rates of MgADP phosphorylation was also determined under similar reaction conditions as above with saturating concentrations of both MgADP (3.5 mM) and carbamoyl phosphate (20 mM) and varying concentrations of free Mg^{2+} (0−11 mM). The dependence of the k_{cat}/K_m for carbamoyl phosphate in the MgADP phosphorylation reaction on pH was also determined under equivalent conditions at

varying pH (5.0–9.0), saturating Mg^{2+} (7.5 mM), and varied concentrations of carbamoyl phosphate (1.2–22.0 mM).

The inhibitory effects of phosphonoacetate with respect to carbamoyl phosphate for the MgADP phosphorylation reaction catalyzed by wild-type *Re*PC were also examined using the same coupled assay system. Initial rates were determined at varying concentrations of carbamoyl phosphate (1.4–28 mM) and fixed concentrations of phosphonoacetate (0.33–20 mM). The 1 mL reactions (pH 7.5, 25 °C) contained 7.5 mM MgCl$_2$, 3.5 mM MgADP, 0.25 mM acetyl-CoA, 0.4 mM glucose, 0.36 mM NADP, glucose-6-phosphate dehydrogenase (5 U), and hexokinase (1U).

Determination of the Coupling of MgATP Cleavage and Pyruvate Carboxylation in the Presence and Absence of Acetyl-CoA. The initial rates of oxaloacetate formation and P$_i$ release were determined at varying concentrations of pyruvate (0.09–5.25 mM) in order to determine the degree of coupling between the two reactions. Two 1 mL reactions containing 15 mM HCO$_3^-$, 5.0 mM MgCl$_2$, 2.5 mM MgATP, and 0.25 mM acetyl-CoA were prepared at each concentration of pyruvate (0.09–5.25 mM). 0.24 mM NADH and malate dehydrogenase (10 U) were added to reactions where oxaloacetate formation was being monitored, and the oxidation of NADH to NAD$^+$ was followed at 340 nm. To reactions where P$_i$ release was being determined, 3 U of PNP and 0.2 mM of MESG were added to the reaction mixtures prior to the addition of *Re*PC (5–10 μg), and the background rate of MESG decomposition was monitored for ~2 min at 360 nm. Reactions were initiated with the addition of *Re*PC, and the corrected rate was used to determine the initial rates of P$_i$ release. Similar reactions were used to determine the extent of coupling in the absence of acetyl-CoA.

Data Analysis. k_{cat} and k_{cat}/K_m values were determined by fitting velocity versus substrate concentration data to eq 1 using least-squares nonlinear regression, where A is the variable substrate concentration. All least-squares fits were performed using FORTRAN programs,[16] and best-fit lines were plotted using SigmaPlot v. 12.0, unless otherwise indicated.

$$v = \frac{V_{max}A}{K_a + A} \tag{1}$$

The initial rates for pyruvate carboxylation determined at varying MgATP concentrations and fixed concentrations of Mg^{2+} were globally fitted to the equilibrium ordered equation

$$v = \frac{V_{max}AB}{K_bA + AB + K_{ia}K_b} \tag{2}$$

where V_{max} is the maximal velocity at saturating concentrations of Mg^{2+} and MgATP, A is the concentration of Mg^{2+}, B is the concentration of MgATP, K_{ia} is the dissociation constant for Mg^{2+}, and K_b is the Michaelis constant for MgATP. When MgATP was saturating and the concentration of pyruvate was varied at fixed concentrations of Mg^{2+} (0.7–3.0 mM), the resulting initial velocity plots were individually fitted to eq 3

$$v = \frac{V(A^2 + dA)}{A^2 + bA + c} \tag{3}$$

where A is the concentration of pyruvate, V is the maximal velocity at saturating pyruvate and the fixed concentration of Mg^{2+}, and b, c, and d are kinetic constants associated with the overall rate of the reaction. Reciprocal plots for the initial rates

of pyruvate carboxylation determined with varying pyruvate and 5 mM of free Mg^{2+} were linear, and the data were fitted to eq 1.

Sigmoidal rate of oxaloacetate formation vs acetyl-CoA curves determined at varying concentrations of Mg^{2+} were individually fitted to eq 4

$$v = \frac{V_{max}(A)^n}{K_a{}^n + A^n} \tag{4}$$

where v is the initial velocity determined, A is the concentration of acetyl-CoA, V_{max} is the maximal velocity at saturating activator concentrations, and n is the Hill coefficient.

k_{cat}/K_m and k_{cat} pH profiles determined for the wild-type *Re*PC-catalyzed carboxylation of pyruvate with MgATP as the variable substrate were fitted to eqs 5 and 6, respectively

$$\log\left(\frac{k_{cat}}{K_m}\right) = \log\left(\frac{C}{1 + \frac{(H^+)}{K_1} + \frac{K_2}{(H^+)} + \frac{K_0}{(H^+)^2}}\right) \tag{5}$$

$$\log k_{cat} = \log\left(\frac{C}{1 + \frac{(H^+)}{K_1} + \frac{K_2}{(H^+)} + \frac{(H^+)^2}{K_0}}\right) \tag{6}$$

where K_1, K_2, and K_0 are the pK_as determined from the fits of the pH profiles, (H$^+$) is the hydrogen ion concentrations corresponding to the pH, and C is a constant. Similarly, k_{cat}/K_m and k_{cat} pH profiles for the full reverse reaction, where MgADP was the variable substrate, were both fitted to eq 7

$$\log\left(\frac{k_{cat}}{K_{m,MgADP}}\right) \text{ or } \log k_{cat} = \log\left(\frac{C}{1 + \frac{(H^+)}{K_1} + \frac{K_2}{(H^+)}}\right) \tag{7}$$

The k_{cat}/K_m pH profile for the phosphorylation of MgADP by the variable substrate, carbamoyl phosphate, was fitted to eq 8

$$\log\left(\frac{k_{cat}}{K_m}\right) = \log\left(\frac{Y_L + \frac{Y_H(K_1)}{(H^+)}}{1 + \frac{K_2}{(H^+)}}\right) \tag{8}$$

where K_1 and K_2 are the pK_as determined from the fit of the k_{cat}/K_m pH profile, (H$^+$) is the hydrogen ion concentrations corresponding to the pH, and Y_L and Y_H are the limiting k_{cat}/K_m values at low and high pH, respectively.

Inhibition of pyruvate carboxylation by phosphonoacetate with respect to MgATP was best described by the linear noncompetitive inhibition equation

$$v = \frac{V_{max}A}{K\left(1 + \frac{I}{K_{is}}\right) + A\left(1 + \frac{I}{K_{ii}}\right)} \tag{9}$$

where V_{max} is the maximal velocity of the uninhibited reaction, A is the concentration of MgATP, I is the concentration of phosphonoacetate, and K_{is} and K_{ii} are the kinetic inhibition constants for the slope and intercept effects, respectively. Inhibition of the phosphorylation of MgADP using carbamoyl phosphate by phosphonoacetate was best described as

Table 1. k_{cat} and k_{cat}/K_m Values Determined for the Various Reactions Catalyzed by Wild-Type RePC[a]

	variable substrate[b]	k_{cat} (min^{-1})	K_m (mM)	k_{cat}/K_m (min^{-1} mM^{-1})	% k_{cat} of pyruvate carboxylation
pyruvate carboxylation	MgATP[c]	396 ± 10[d]	0.145 ± 0.009	2670 ± 120	(100)
	HCO$_3^-$	700 ± 20	10.8 ± 0.4	64.8 ± 0.9	
	pyruvate	440 ± 8[d]	0.15 ± 0.01	2900 ± 150	
full reverse reaction	MgADP	0.835 ± 0.005	0.12 ± 0.02	6.95 ± 0.002	0.2
oxamate-induced decarboxylation of oxaloacetate	ND[e]	9.03 ± 0.04[f]			2.0
HCO$_3^-$- dependent ATPase	MgATP	2.58 ± 0.09	0.022 ± 0.003	115 ± 2	0.6
ADP phosphorylation	carbamoyl phosphate	2.41 ± 0.01	2.6 ± 0.5	0.93 ± 0.02	0.6
	acetyl phosphate	0.56 ± 0.02	0.34 ± 0.02	1.70 ± 0.05	0.1

[a]Kinetic parameters were determined from data fits to eq 1. [b]Varied substrate indicated; all other substrates were held constant at saturating concentrations. Reaction conditions: 50 mM Bis-tris, 25 mM tricine, 25 mM glycine (pH 7.5), 25 °C, 0.25 mM acetyl-CoA. For more detailed reaction conditions see Methods section. [c]k_{cat} (min^{-1}) and k_{cat}/K_m (min^{-1} mM^{-1}) were determined from fits of the initial rates of pyruvate carboxylation at varying concentrations of MgATP and fixed Mg^{2+} to the equation for an equilibrium ordered pattern (eq 2) and the $K_{ia,Mg^{2+}}$ = 1.2 ± 0.2 mM. All other k_{cat} and k_{cat}/K_m values were determined from fits to eq 1. [d]Apparent k_{cat}. [e]ND = not determined. [f]Specific activity, determined in triplicate with saturating concentrations of all substrates and activators.

hyperbolic noncompetitive inhibition (eq 10)

$$v = \frac{V_{max}(A)\left(1 + \dfrac{I}{K_{id}}\right)}{K\left(1 + \dfrac{I}{K_{is}}\right) + A\left(1 + \dfrac{I}{K_{ii}}\right)} \quad (10)$$

where V_{max} is the maximal velocity of the uninhibited reaction, A is the concentration of carbamoyl phosphate, I is the concentration of phosphonoacetate, and K_{id}, K_{is}, and K_{ii} are the kinetic inhibition constants for the partial inhibition, slope, and intercept effects, respectively.

■ RESULTS

Kinetic Characterization of Wild-Type PC from R. etli. k_{cat} and k_{cat}/K_m values were determined for wild-type RePC for various substrates in the forward and reverse reactions in the presence of saturating concentrations of Mg^{2+} and acetyl-CoA (Table 1). The kinetic characterization revealed that the relative rates and catalytic efficiencies for the full reverse and partial forward and reverse reactions of the BC and CT domains were substantially lower than those determined for the wild-type-catalyzed carboxylation of pyruvate. The rate of oxaloacetate decarboxylation and subsequent formation of MgATP (full reverse reaction) was only 0.2% of the rate of pyruvate carboxylation, resulting in a nearly 400-fold difference between the k_{cat}/K_m determined for MgATP and MgADP in the forward and reverse reactions, respectively. The relative rate of oxaloacetate decarboxylation in the presence of oxamate was determined to be 2.0% of the full forward reaction. Compared to the rate of the full reverse reaction, saturating oxamate concentrations stimulated the rate of oxaloacetate decarboxylation in the CT domain 11-fold. Reactions occurring strictly in the BC domain also exhibited rates and catalytic efficiencies significantly lower than those for the full forward reaction. The HCO$_3^-$-dependent ATPase reaction was nearly 180-fold slower than the overall forward reaction. A considerable decrease in the observed K_m for MgATP was accompanied by a 20-fold decrease in the $k_{cat}/K_{m,MgATP}$ for the MgATP-hydrolysis compared to the $k_{cat}/K_{m,MgATP}$ for pyruvate carboxylation. While the catalytic rate of MgADP phosphorylation by carbamoyl phosphate was equivalent to the rates of MgATP hydrolysis, acetyl phosphate was found to be a considerably slower substrate than carbamoyl phosphate (0.1% of the rate of

pyruvate carboxylation). Interestingly, the rate of the partial reverse reaction of the BC domain using carbamoyl phosphate as a substrate was 3 times greater than the rates of the full reverse reaction while the rate with acetyl phosphate as a substrate was 1.5 times less than the full reverse reaction. An accurate determination of the k_{cat}/K_m for HCO$_3^-$ under CO$_2$-free conditions with saturating concentrations of free Mg^{2+} (5 mM) revealed a relatively high K_m for HCO$_3^-$ of 10.8 ± 0.4 mM and a k_{cat} of 700 ± 20 min^{-1} (Figure S1).

Effects of Mg^{2+} on Pyruvate Carboxylation and MgADP Phosphorylation. To determine the mechanistic role of free Mg^{2+} in the wild-type-catalyzed carboxylation of pyruvate, Mg^{2+} was treated as a pseudoreactant[17] and initial velocity patterns for Mg^{2+} vs MgATP, Mg^{2+} vs pyruvate, and Mg^{2+} vs acetyl-CoA were determined. The intersecting initial velocity pattern observed in the Mg^{2+} vs MgATP plots (Figure S2) indicates that Mg^{2+} and MgATP add to the BC domain in rapid equilibrium with Mg^{2+} binding first. The dissociation constant for Mg^{2+} (K_{ia}), determined from global fits of the data to eq 2, was 1.2 ± 0.2 mM while the K_b for MgATP was 0.145 ± 0.009 mM. Increasing amounts of free Mg^{2+} also activated the phosphorylation of MgADP by carbamoyl phosphate, resulting in a linear increase in k_{cat} (Figure S3). While high concentrations of free Mg^{2+} (>7 mM) inhibited pyruvate carboxylation and MgATP cleavage, there was no inhibition of the MgADP phosphorylation reaction by Mg^{2+} (up to 11 mM).

The initial velocities of the wild-type-catalyzed carboxylation of pyruvate were also measured at several fixed concentrations of free Mg^{2+} and varying concentrations of pyruvate (Figure 1A). Nonlinear, concave downward reciprocal plots were observed at Mg^{2+} concentrations of 0.7−3.0 mM. Kinetic parameters determined from individual fits of these data to eq 3 show that Mg^{2+} had a significant effect on the rate of pyruvate carboxylation but only a marginal effect on the K_m for pyruvate (Table 2). At 5 mM free Mg^{2+}, the reciprocal plot was linear, and the data were fitted to eq 1. A replot of the apparent $1/V_{max}$ vs $1/[Mg^{2+}]$ (Figure 1B) was used to estimate the K_a for Mg^{2+} for the effect on V_{max} (≈40 mM). Similarly, the effects of free Mg^{2+} on the activation of the pyruvate carboxylation reaction by acetyl-CoA was determined by measuring the initial rates of oxaloacetate formation at varying concentrations of acetyl-CoA and fixed concentrations of Mg^{2+} (Figure 2). Kinetic parameters determined from individual fits of the data to eq 4 show that
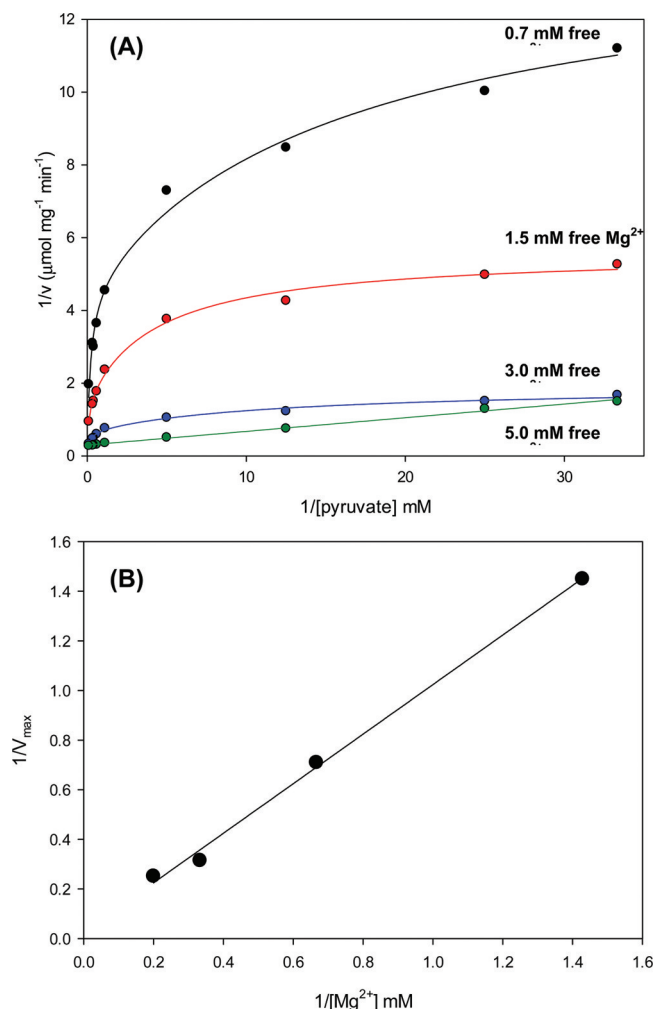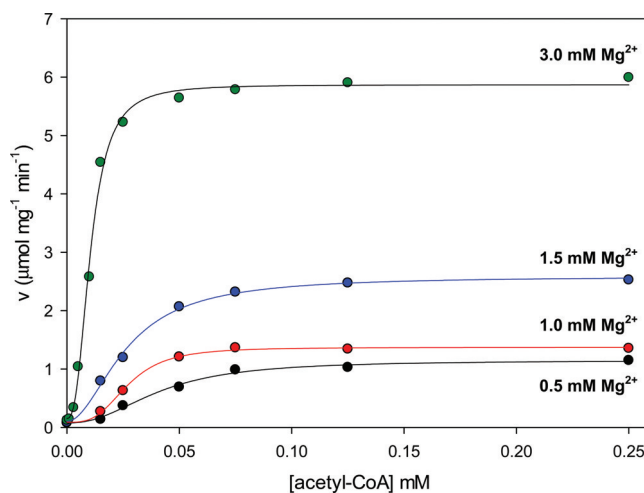
Figure 2. Initial rates of pyruvate carboxylation at varied concentrations of acetyl-CoA (0−0.25 mM) and fixed concentrations of free Mg^{2+} (0.5 mM, black; 1.0 mM, red; 1.5 mM, blue; 3.0 mM, green). Solid lines indicate the least-squares individual fits to the Hill equation (eq 4).

Table 3. Kinetic Parameters Determined from Measuring the Initial Rates of Pyruvate Carboxylation with Varying Concentrations of Acetyl-CoA at Fixed Concentrations of Free Mg^{2+} [a]

	V_{max} (μmol mg^{-1} min^{-1})	$K_{a,acetyl\text{-}CoA}$ (μM)	$n_{acetyl\text{-}CoA}$
0.5 mM Mg^{2+}	1.16 ± 0.07	38 ± 2	2.0 ± 0.3
1.0 mM Mg^{2+}	1.39 ± 0.06	26 ± 2	2.8 ± 0.5
1.5 mM Mg^{2+}	2.59 ± 0.08	25 ± 1	1.8 ± 0.2
3.0 mM Mg^{2+}	5.7 ± 0.1	10.0 ± 0.4	2.6 ± 0.2

[a]Kinetic parameters were determined from data fits to eq 4.

Figure 1. (A) Nonlinear double-reciprocal plots obtained when the initial rates of pyruvate carboxylation were determined at varying concentrations of pyruvate (0.03−10 mM) and fixed concentrations of free Mg^{2+} (0.7 mM, black; 1.5 mM, red; 3.0 mM, blue; 5.0 mM, green). Solid lines are the calculated individual fits of the data to eq 3 for Mg^{2+} concentrations up to 3.0 mM and to eq 1 for 5.0 mM Mg^{2+}. (B) Replot of V_{max} vs $1/[Mg^{2+}]$.

Table 2. Kinetic Parameters Determined from Measuring the Initial Rates of Pyruvate Carboxylation with Varying Concentrations of Pyruvate at Fixed Concentrations of Free Mg^{2+} [a]

	V_{max} (μmol mg^{-1} min^{-1})	$K_{m,pyruvate}$ (mM)	$V/K_{m,pyruvate}$
0.7 mM Mg^{2+}	0.69 ± 0.02	3.1 ± 0.2	0.22 ± 0.03
1.5 mM Mg^{2+}	1.41 ± 0.01	3.0 ± 0.4	0.47 ± 0.08
3.0 mM Mg^{2+}	3.18 ± 0.08	2.65 ± 0.04	1.2 ± 0.7
5.0 mM Mg^{2+}	3.98 ± 0.04	0.15 ± 0.01	27.3 ± 0.5

[a]Kinetic parameters were determined from data fits to eq 1 or eq 3.

increasing concentrations of Mg^{2+} had little effect on the sigmoidicity of the curves, indicated by the relatively minor variations in the determined Hill coefficients (Table 3). A steady increase in the rate of pyruvate carboxylation was observed with increasing concentrations of Mg^{2+}, demonstrated most clearly in the observed 4.9-fold increase in k_{cat} when concentrations of Mg^{2+} were increased from 0.5 to 3 mM. Small but significant decreases in the K_a for acetyl-CoA were observed at increasing Mg^{2+} concentrations up to 1.5 mM (K_a = 38−25 μM). An

overall 3.8-fold decrease in the K_a for acetyl-CoA (10 μM) was determined with the addition of 3.0 mM free Mg^{2+}.

Dependence of Pyruvate Carboxylation, Oxaloacetate Decarboxylation, and MgADP Phosphorylation on pH. The dependence of k_{cat} and k_{cat}/K_m on pH in the full forward and reverse reactions was examined for the wild-type *Re*PC-catalyzed reactions (Figure 3). When MgATP was the variable substrate, the k_{cat}/K_m pH profile for pyruvate carboxylation decreased at both high and low pH with pK_as at ∼8.0. The k_{cat} pH profile for pyruvate carboxylation showed three pK_as at 6.6, 7.4, and 8.5. In the reverse reaction, MgADP was varied while phosphate and oxaloacetate were held at fixed saturating concentrations. While the k_{cat}/K_m and k_{cat} profiles appear deceptively flat, both sets of data were satisfactorily fitted to eq 7 (σ = 0.04), revealing two pK_as near 5.2 and 9.4. Because of the instability of *Re*PC at a pH less than 6 or greater than 8.5, the profile could not be extended further. The phosphorylation of MgADP, with carbamoyl phosphate as the varied substrate, exhibited only a partial dependence on pH and fits of the k_{cat}/K_m data to eq 8 revealed pK_as of 7.7 and 6.9 (Figure 3C). The k_{cat} for the phosphorylation MgADP by carbamoyl phosphate was pH independent (data not shown).

Effects of Acetyl-CoA on Wild-Type *Re*PC Activities and the Coupling of the BC and CT Domain Reactions. Specific activities for each of the *Re*PC-catalyzed reactions were determined in the presence and absence of saturating concentrations of acetyl-CoA (Table 4). Acetyl-CoA had the greatest effect on the rate of pyruvate carboxylation, and its
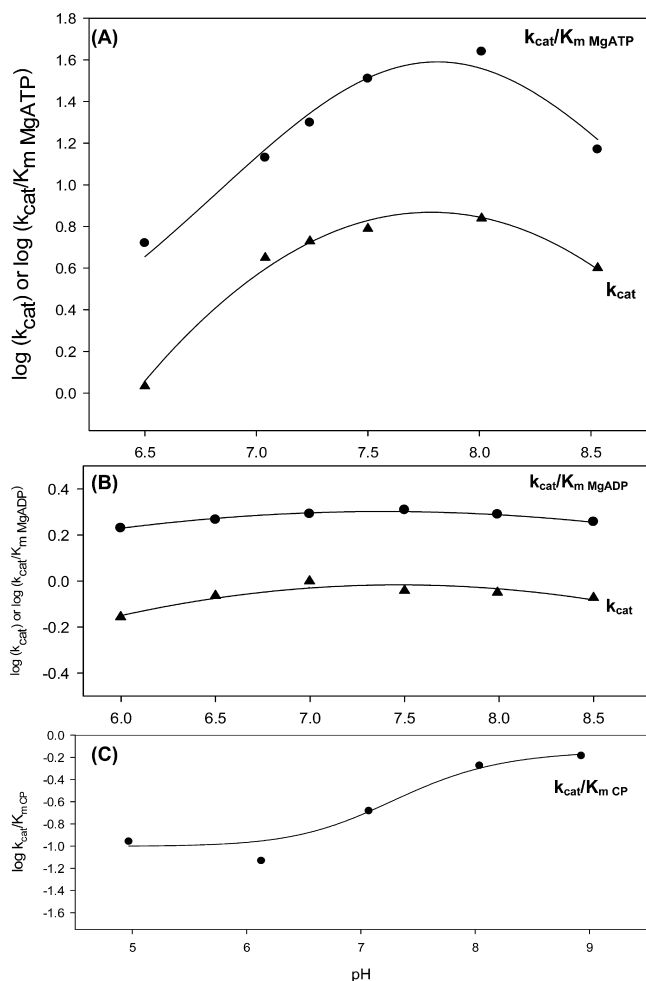
Figure 3. pH profiles for the pyruvate carboxylation reaction (A), full reverse reaction (B), and MgADP phosphorylation reaction (C) catalyzed by wild-type *Re*PC. (A) For the dependence of k_{cat}/K_m for pyruvate carboxylation on pH, $pK_1 = 8.0 \pm 0.1$, $pK_2 = 8.09 \pm 0.01$, and $pK_0 - pK_2 = 8.2 \pm 0.5$ values were obtained with MgATP as the variable substrate and data fits to eq 5. k_{cat} data were fitted to eq 6, and values of $pK_1 = 6.6 \pm 0.8$, $pK_2 = 8.5 \pm 0.2$, and $pK_0 - pK_2 = 7.4 \pm 0.2$ were obtained. (B) Two pK_as were observed in both the $k_{cat}/K_{m,MgADP}$ ($pK_1 = 5.2 \pm 0.1$ and $pK_2 = 9.5 \pm 0.2$) and k_{cat} ($pK_1 = 5.30 \pm 0.08$ and $pK_2 = 9.4 \pm 0.1$) pH profiles for the full reverse reaction (eq 7). (C) The pH had only a partial effect on phosphorylation of MgADP by carbamoyl phosphate, and the k_{cat}/K_m pH profile showed two pK_as ($pK_1 = 6.9 \pm 0.2$ and $pK_2 = 7.7 \pm 0.2$) with carbamoyl phosphate was the variable substrate. Data were fitted to eq 8.

absence resulted in catalytic activities that were only 9% of the fully activated enzyme. The lack of acetyl-CoA also caused fairly drastic decreases in the rates of both MgATP hydrolysis and the full reverse reaction (82% and 78%, respectively). Acetyl-CoA also had a noticeable effect on the activity of the oxamate-induced decarboxylation of oxaloacetate but no effect on the rate of MgADP phosphorylation by carbamoyl phosphate.

To assess the extent of coupling between MgATP cleavage in the BC domain and carboxyl transfer in the CT domain, the rates of P$_i$ release and oxaloacetate formation were measured under identical reaction conditions with varying amounts of pyruvate in the presence and absence of acetyl-CoA (Figure 4). The rates of both reactions exhibited a hyperbolic dependence on the concentration of pyruvate in the presence of saturating acetyl-CoA (Figure 4A), and kinetic parameters were

Table 4. Effect of Acetyl-CoA on the Activities of Wild-Type-Catalyzed Reactions[a]

	(+) acetyl-CoA	(−) acetyl-CoA	
	k_{cat} (min^{-1})[b]	k_{cat} (min^{-1})	% rate[c]
pyruvate carboxylation	700 ± 20	65.8 ± 0.4	9
full reverse reaction	0.835 ± 0.005	0.152 ± 0.03	18
HCO$_3^-$-dependent ATPase	2.58 ± 0.09	0.547 ± 0.002	22
oxamate-induced decarboxylation of oxaloacetate	9.03 ± 0.04	6.00 ± 0.05	67
ADP phosphorylation	2.4 ± 0.1	2.43 ± 0.01	100

[a]For detailed reaction conditions see Methods section. [b]Specific activities were determined for each reaction, with saturating concentrations of all substrates, in triplicate. Errors reported are the standard deviations from those determinations. [c]Compared to the specific activity in the presence of acetyl-CoA.
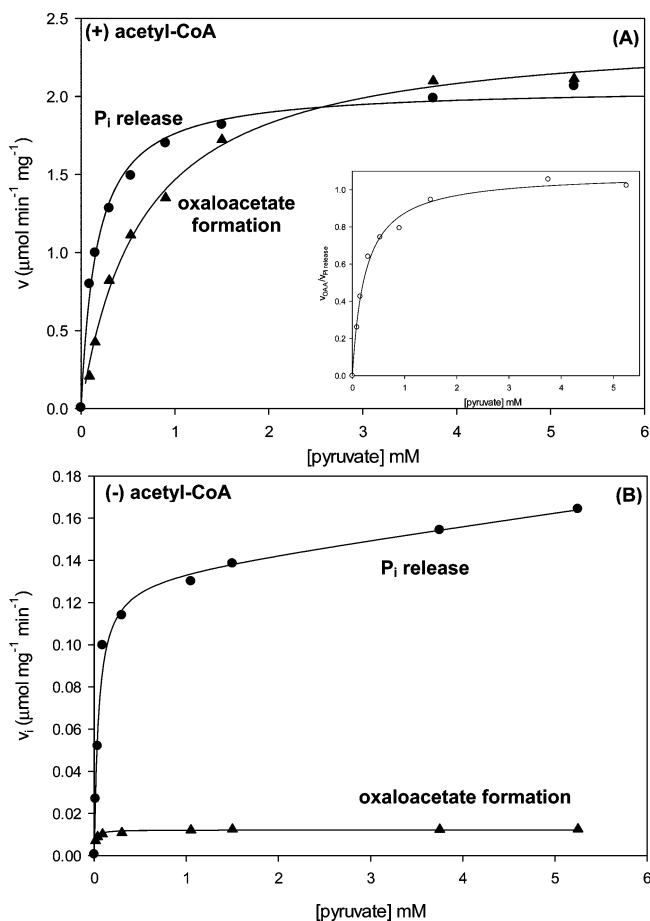

Figure 4. Initial rates of P$_i$ release (●) and oxaloacetate formation (▲) at varying concentrations of pyruvate (0.03–5.25 mM) were determined to evaluate the extent of coupling between the HCO$_3^-$-dependent ATP cleavage and pyruvate carboxylation reactions in the presence (A) and absence (B) of saturating concentrations of acetyl-CoA. Solid lines indicate the least-squares fits to eq 1. Inset: ratio of the rates of oxaloacetate formation and P$_i$ release (○) as a function of pyruvate concentrations. Solid lines indicate the least-squares fits to eq 1.

determined from fits of the data to eq 1 (Table 5). The K_a of pyruvate for the stimulation of P$_i$ release was determined to be 0.16 ± 0.01 mM while the K_m of pyruvate determined for the oxaloacetate formation was 4-fold greater. The decreased K_a for pyruvate for the stimulation of P$_i$ release partially accounts

Table 5. Effect of Acetyl-CoA on the Coupling of the HCO₃⁻-Dependent ATPase Reaction in the BC Domain to Pyruvate Carboxylation in the CT Domain[a]

	(+) acetyl-CoA	(−) acetyl-CoA	% of (+) acetyl-CoA[b]
P_i release[c]			
k_{cat} (min⁻¹)	290 ± 5	16.9 ± 0.8	5.8
$K_{a,pyruvate}$ (mM)	0.16 ± 0.01	0.048 ± 0.008	30
k_{cat}/K_a (min⁻¹ mM⁻¹)	1820 ± 10	350 ± 15	19
oxaloacetate formation			
k_{cat} (min⁻¹)	310 ± 8	1.52 ± 0.03	0.5
$K_{m,pyruvate}$ (mM)	0.65 ± 0.05	0.013 ± 0.002	2
k_{cat}/K_m (min⁻¹ mM⁻¹)	470 ± 15	115 ± 5	24

[a]Initial rates of P_i release and oxaloacetate formation were determined as detailed in the Methods section in both the presence and absence of 0.25 mM acetyl-CoA at varying concentrations of pyruvate (0.03−5.25 mM) and 15 mM HCO₃⁻. [b]Percentage of parameters determined without acetyl-CoA compared to those determined with acetyl-CoA. [c]Kinetic parameters were determined from fits of the data to eq 1.

Table 6. Effect of Free Biotin on the Kinetic Parameters for the HCO₃⁻-Dependent ATPase Reaction Catalyzed by the Wild-Type and Mutant Forms of *Re*PC[a]

					(+) 10 mM free biotin			
	k_{cat} (min⁻¹)[b]	$K_{m,MgATP}$ (mM)	k_{cat}/K_m (min⁻¹ mM⁻¹)	% wild-type k_{cat}/K_m	k_{cat} (min⁻¹)	K_m (mM)	k_{cat}/K_m (min⁻¹ mM⁻¹)	% wild-type k_{cat}/K_m
wild-type	2.58 ± 0.09	0.022 ± 0.003	115 ± 2	(100)	3.02 ± 0.01	0.018 ± 0.007	167 ± 5	(100)
K1119Q	0.082 ± 0.001	1.20 ± 0.7	0.068 ± 0.005	0.06	2.69 ± 0.06	0.040 ± 0.001	67.5 ± 0.3	40
T882A	14 ± 2	0.054 ± 0.002	260 ± 15	225	38 ± 7	0.09 ± 0.05	430 ± 10	260

[a]Reaction conditions: 50 mM Bis-Tris, 25 mM tricine, 25 mM glycine (pH 7.5), 25 °C, 15 mM HCO₃⁻, 10 mM biotin, 7.5 mM MgCl₂, MgATP (0.09−3.0 mM), 0.25 mM acetyl-CoA. [b]Data fitted to eq 1.

for the 3.7-fold increase in the k_{cat}/K_a compared to that determined when measuring the rate of oxaloacetate formation. A plot of the ratio of the rates of oxaloacetate formation to the rates of P_i release vs pyruvate concentrations (Figure 4A inset) revealed a K_a for pyruvate of 0.25 mM and a limiting value of the ratio to be 1.08, indicating the complete coupling between the HCO₃⁻-dependent MgATP cleavage in the BC domain and oxaloacetate formation in the CT domain at saturating concentrations of pyruvate. While the ratio of the initial rates of oxaloacetate formation and P_i release did not reach 1:1 until concentrations of pyruvate ≈1 mM, a 300−500-fold stimulation of the rate of P_i release from the BC domain was observed at the lowest concentrations of pyruvate in the presence of acetyl-CoA.

In the absence of acetyl-CoA (Figure 4B), the initial rates of oxaloacetate formation were fitted to eq 1, giving a K_m for pyruvate of 0.013 ± 0.002 mM, which was 50-fold lower than that determined in the presence of acetyl-CoA and 3.7-fold lower than the K_a of pyruvate determined for the stimulation of P_i release in the absence of acetyl-CoA (Table 5). The K_a for the pyruvate stimulation of the rates of P_i release in the absence of acetyl-CoA displayed a 3-fold decrease compared to the K_a determined with saturating acetyl-CoA. The 11-fold increase in the k_{cat} for P_i release compared to oxaloacetate formation indicates a nearly complete lack of coupling between MgATP-hydrolysis and pyruvate carboxylation at saturating concentrations of pyruvate. In the absence of acetyl-CoA, the presence of low concentrations of pyruvate still resulted in a significant stimulation (120−175-fold increase) of the rates of P_i release from the BC domain.

Effects of Free Biotin on the BC Domain Reactions. The activation of the catalytic reactions occurring in the BC

domain by free biotin were examined with a tetrameric enzyme that lacks tethered biotin (K1119Q mutant,[9,18]), a tetrameric holoenzyme where positioning of the tethered biotin favors placement in the BC domain (T882A mutant,[9]), and with the tetrameric wild-type holoenzyme. The effect of 10 mM free biotin on the kinetic parameters for the wild-type-, T882A-, and K1119Q *Re*PC-catalyzed HCO₃⁻-dependent ATPase reaction is shown in Table 6. Free biotin increases the k_{cat} for both the wild-type and the T882A *Re*PC-catalyzed reactions without having a major effect on the K_m for MgATP. In the K1119Q-catalyzed reaction, the addition of 10 mM biotin increases the k_{cat} of MgATP hydrolysis to rates observed for wild-type *Re*PC in the absence of free biotin. This rate increase, coupled with a 35-fold decrease in the K_m for MgATP, results in a nearly 1000-fold increase in the catalytic efficiency of the K1119Q *Re*PC-catalyzed reaction when 10 mM free biotin is added.

The effect of free biotin on the *Re*PC-catalyzed phosphorylation of MgADP using either carbamoyl phosphate or acetyl phosphate as a phosphoryl donor (Table 7) was also examined. While the overall rate of the wild-type-catalyzed phosphorylation of MgADP was 4 times slower with acetyl phosphate as the phosphoryl donor, a significant decrease in the K_m for acetyl phosphate, compared to carbamoyl phosphate, resulted in a k_{cat}/K_m value nearly twice that for carbamoyl phosphate in the absence of free biotin. The addition of 10 mM biotin to the wild-type-catalyzed reactions increased the k_{cat} of the phosphorylation of MgADP by carbamoyl phosphate but inhibited the rate of phosphorylation by acetyl phosphate. The T882A-catalyzed rate of MgADP phosphorylation with carbamoyl phosphate in the absence and presence of 10 mM biotin was 10 and 7.8 times greater, respectively, than the rate of the wild-type-catalyzed reactions. In contrast, the rate of the

Table 7. Activities of the Wild-Type and Mutant *Re*PC for the MgADP Phosphorylation Reaction Using Either Carbamoyl Phosphate or Acetyl Phosphate in the Presence and Absence of Biotin[a]

	k_{cat} (min^{-1})[b]	K_m (mM)	k_{cat}/K_m (min^{-1} mM^{-1})	% wild-type k_{cat}/K_m	(+) 10 mM free biotin k_{cat} (min^{-1})	K_m (mM)	k_{cat}/K_m (min^{-1} mM^{-1})	% wild-type k_{cat}/K_m
carbamoyl phosphate[c]								
wild-type	2.4 ± 0.1	2.6 ± 0.5	0.93 ± 0.02	(100)	4.1 ± 0.3	3.3 ± 0.5	1.2 ± 0.1	(100)
K1119Q	0.014 ± 0.001	0.88 ± 0.07	0.16 ± 0.01	17	2.1 ± 0.1	3.9 ± 0.6	0.54 ± 0.06	45
T882A	24 ± 1	3.4 ± 0.5	7.0 ± 0.6	750	32.1 ± 0.8	2.9 ± 0.2	11 ± 1	920
acetyl phosphate[d]								
wild-type	0.58 ± 0.01	0.34 ± 0.02	1.70 ± 0.05	(100)	0.29 ± 0.002	0.14 ± 0.04	2.1 ± 0.2	(100)
K1119Q	0.47 ± 0.01	0.29 ± 0.01	1.62 ± 0.05	95	0.44 ± 0.01	0.37 ± 0.03	1.19 ± 0.02	57
T882A	0.30 ± 0.01	0.22 ± 0.01	1.36 ± 0.01	80	0.12 ± 0.01	0.14 ± 0.01	0.85 ± 0.03	40

[a]Reaction conditions: 50 mM Bis-Tris, 25 mM tricine, 25 mM glycine (pH 7.5), 25 °C, 7.5 mM MgCl$_2$, 3.5 mM MgADP, 0.25 mM acetyl-CoA. [b]Data fitted to eq 1. [c]Carbamoyl phosphate varied phosphoryl donor (1−20 mM). [d]Acetyl phosphate varied phosphoryl donor (0.1−20 mM).

T882A-catalyzed phosphorylation with acetyl phosphate was significantly lower than the wild-type rate of MgADP phosphorylation with acetyl phosphate. The addition of 10 mM free biotin reduced the rate of the T882A-catalyzed phosphorylation with acetyl phosphate even further.

Comparable to the effects observed for wild-type *Re*PC, the T882A *Re*PC mutant also exhibited a significantly reduced K_m for acetyl phosphate when compared to carbamoyl phosphate, in both the presence and absence of 10 mM biotin. The K1119Q *Re*PC mutant catalyzed the phosphorylation of MgADP using acetyl phosphate as the phosphoryl donor at rates comparable to wild-type *Re*PC in the absence of free biotin. Despite effectively increasing the rates of MgADP phosphorylation with carbamoyl phosphate as the substrate, free biotin had only small effects on the k_{cat} and k_{cat}/K_m when acetyl phosphate was the phosphoryl donor in the K1119Q mutant catalyzed reaction.

Inhibition of Pyruvate Carboxylation and MgADP Phosphorylation by Phosphonoacetate. Phosphonoacetate,
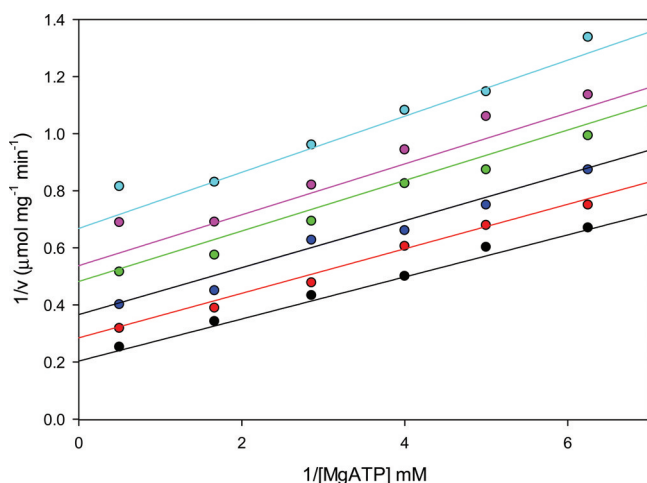

Figure 5. Linear, noncompetitive inhibition of pyruvate carboxylation by phosphonoacetate with respect to MgATP. Initial rates were determined at varying concentrations of MgATP (0.16−2.0 mM) and fixed concentrations of phosphonoacetate (0 mM, black; 1.05 mM, red; 2.10 mM, blue; 3.6 mM, green; 4.2 mM, pink; 6.0 mM, cyan). Data were fitted to eq 9, and the solid lines indicate the least-squares fits to the equation. Kinetic parameters from these fits are shown in Table 8.

an isosteric and isoelectronic analogue of the putative carboxyphosphate intermediate, is an effective inhibitor of pyruvate carboxylation (Figure 5) and MgADP phosphorylation with carbamoyl phosphate (Figure 6) in the wild-type
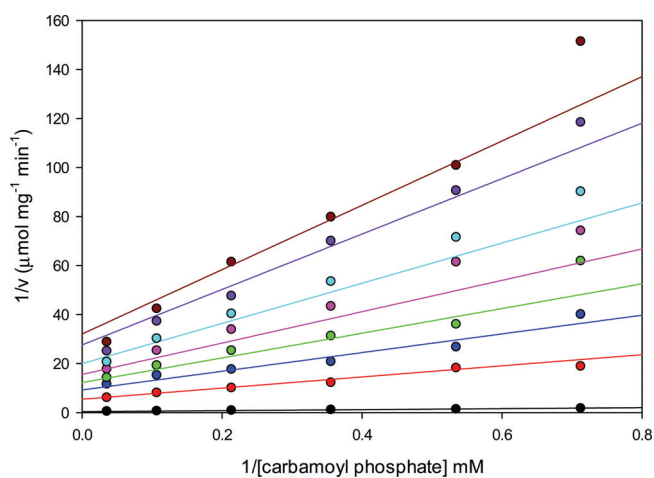

Figure 6. Hyperbolic, noncompetitive inhibition of the ADP phosphorylation reaction by phosphonoacetate with respect to carbamoyl phosphate. Initial rates were determined at varying concentrations of carbamoyl phosphate (1.4−20 mM) and fixed concentrations of phosphonoacetate (0 mM, black; 0.33 mM, red; 0.66 mM, blue; 1.0 mM, green; 1.5 mM, pink; 2.5 mM, cyan; 7.0 mM, purple; 20 mM, dark red). Data were fitted to eq 10, and the solid lines indicate the least-squares fits to the equation. Kinetic parameters from these fits are presented in Table 8.

*Re*PC reactions. Inhibition of pyruvate carboxylation with respect to MgATP by phosphonoacetate was noncompetitive, and kinetic parameters determined from global fits of the data to eq 9 are shown in Table 8. Kinetic parameters for the partial inhibition of MgADP phosphorylation by phosphonoacetate (Figure 6) were best defined from global fits of the data to eq 10 describing hyperbolic, noncompetitive inhibition (Table 8). While only a partial inhibitor of the phosphorylation reaction, saturating concentrations of phosphonoacetate (K_{id} = 1.9 ± 0.3 mM) would result in nearly complete inhibition, with V_{max} and V/K_m values only 1% and 1.5% of the uninhibited catalytic reaction. The virtually identical slope and intercept inhibition

Table 8. Inhibition of Pyruvate Carboxylation and MgADP Phosphorylation by Phosphonoacetate with Respect to MgATP or Carbamoyl Phosphate

pyruvate carboxylation[a]		ADP phosphorylation[b]	
k_{cat} (min^{-1})	620 ± 25	k_{cat} (min^{-1})	3.25 ± 0.02
K_m (mM)	0.36 ± 0.03	K_m (mM)	5.20 ± 0.06
K_{is} (mM)	2.6 ± 0.3	K_{is} (mM)	0.027 ± 0.003
K_{ii} (mM)	18 ± 7	K_{ii} (mM)	0.021 ± 0.001
		K_{id} (mM)	1.9 ± 0.3

[a]Data were fitted to eq 9 with MgATP as the variable substrate. [b]Data were fitted to eq 10 describing hyperbolic noncompetitive inhibition with respect to carbamoyl phosphate.

constants (K_{is} = 0.027 ± 0.003 mM and K_{ii} = 0.021 ± 0.001 mM) determined for the inhibition of MgADP phosphorylation by phosphonoacetate were 100-fold and 890-fold lower than similar inhibition constants determined for the phosphonoacetate inhibition of the pyruvate carboxylation reaction (K_{is} = 2.6 ± 0.3 mM and K_{ii} = 18 ± 7 mM).

■ DISCUSSION

Comparison of the Kinetic Parameters for PC from *R. etli* with PC from Other Sources. The rate of the wild-type *Re*PC-catalyzed oxaloacetate decarboxylation and subsequent formation of MgATP was only 0.2% of the rate of pyruvate carboxylation. Compared to the relative rates of the full forward and reverse reactions catalyzed by PC isolated from sheep[19] and chicken liver,[20,21] the rate of decarboxylation is significantly lower in *Re*PC compared to the rate of carboxylation. This suggests that *Re*PC may be designed to minimize the reversibility of the catalytic carboxylation of pyruvate. Detailed further in the two accompanying articles,[7,13] the formation of a distinct salt bridge between Arg353 and Glu248 near the opening of the BC domain may preclude the access of carboxybiotin to the active site, effectively reducing the relative rate of carboxybiotin decarboxylation in the reverse reaction. Further, the rate of the *Re*PC-catalyzed oxamate-stimulated decarboxylation of oxaloacetate was 2.0% of the full forward reaction, suggesting that an additional partially rate-limiting step may exist in the BC domain which influences the rate of the full reverse reaction.

To the best of our knowledge, acetyl phosphate has not been previously shown to be a suitable phosphoryl donor for the PC-catalyzed phosphorylation of MgADP. While the k_{cat}/K_m for the wild-type-catalyzed reaction with acetyl phosphate was almost twice that determined with carbamoyl phosphate as the substrate, the decreased k_{cat} and K_m for acetyl phosphate implies that the release of products is more rate-limiting compared to when carbamoyl phosphate is the substrate. The T882A *Re*PC mutant also catalyzes the MgADP phosphorylation reaction with acetyl phosphate as a phosphoryl donor. The activating effect the T882A mutation has on the phosphorylation reaction with carbamoyl phosphate as the substrate, most likely due to the increased presence of the tethered biotin in the BC domain,[9] is not observed when acetyl phosphate is used as the phosphoryl donor. In fact, the rate of the T882A *Re*PC-catalyzed phosphorylation of MgADP with acetyl phosphate was actually 52% less than that determined for the wild-type-catalyzed reaction. This observation, coupled with the slight inhibitory effect of free biotin on the k_{cat} for MgADP phosphorylation in the T882A *Re*PC mutant, could indicate that binding of acetyl phosphate in the BC domain disfavors

the binding of tethered or free biotin in the active site. Computational docking studies[13] show that acetyl phosphate adopts a conformation similar to carbamoyl phosphate in the active site which places the hydrophobic acetyl group near the biotin binding pocket.

The T882A *Re*PC crystal structure cocrystallized with phosphonoacetate[13] also shows that phosphonoacetate can adopt multiple, energetically favorable conformations in the BC domain, specifically one where the phosphoryl group is positioned toward ADP and the other with the carboxyl-moiety is positioned toward ADP and near the Mg^{2+} center in the active site. This isosteric and isoelectronic inhibitory analogue of the carboxyphosphate intermediate[22] is a noncompetitive inhibitor of pyruvate carboxylation and a partial noncompetitive inhibitor of the phosphorylation of MgADP with carbamoyl phosphate. Previous studies with sheep kidney PC have also shown that phosphonoacetate is a noncompetitive inhibitor with respect to MgATP for the full forward reaction with a K_i of 0.5 mM.[22] The nearly identical values of K_{ii} and K_{is} for phosphonoacetate determined for the inhibition of the phosphorylation reaction signifies the ability of phosphonoacetate to inhibit the activity equally as well in the presence or absence of carbamoyl phosphate. Presumably, the second Mg^{2+} in the BC domain active site will have available coordination sites that can be occupied by the carboxylic end of phosphonoacetate prior to the formation of MgATP in the reaction, resulting in the significant inhibition by phosphonoacetate in the absence of carbamoyl phosphate in the active site. In the presence of carbamoyl phosphate, phosphonoacetate still remains a potent inhibitor of the phosphorylation reaction. This, coupled with the noncompetitive nature of the inhibition of the full forward reaction with respect to MgATP in both *Re*PC and in sheep kidney PC,[22] could indicate that phosphonoacetate may also bind in the position in the active site normally occupied by the γ-phosphoryl group of MgATP.

pH Variation of the BC Domain Reactions of PC Reveals the Possible Protonation State of the Active Site Base. Previous studies have shown that the oxamate-induced decarboxylation of oxaloacetate in the CT domain is pH independent in avian PC.[21] The proposed mechanism for pyruvate carboxylation in the CT domain of *Re*PC, facilitated by a strictly conserved Thr residue,[9] also suggests similar pH independence would be observed with the *Re*PC enzyme. Therefore, the pH profiles for the overall forward and reverse reactions (Figure 3) are likely to reflect the pH dependence of reactions in the BC domain. In the forward reaction, the HCO$_3^-$-dependent cleavage of MgATP and subsequent carboxylation of the tethered biotin would result in the formation of MgADP, HPO$_4^{2-}$, and the enzyme−biotin−CO$_2^-$ complex as products and the generation of a single proton due to the initial deprotonation of HCO$_3^-$. In the profiles where the concentrations of the nucleotides (either MgATP or MgADP) were varied, the pKs reflect those present in the enzyme−Mg^{2+} complex while the profile for the MgADP phosphorylation reaction, where the concentration of carbamoyl phosphate was varied, reveals the pK_as present in the enzyme−Mg^{2+}−MgADP complex.

While only speculative, the assignment of one of the pK_as in the pH profiles to Glu305 agrees with the proposed catalytic function of this residue. Contained within the hydrogen-bonded catalytic triad composed of strictly conserved residues (Lys245-Glu305-Glu218), Glu305 is proposed to act as the active site base responsible for the deprotonation of HCO$_3^-$

(Scheme 2). If this is the role of Glu305 in the catalytic mechanism, then it must remain ionized prior to the deprotonation of HCO_3^- in the forward reaction. The low side pKs observed in all the pH profiles indicate that the protonation of some residue in the active site appears to prevent catalysis in the forward and reverse reactions and reduces the catalytic activity in the otherwise pH-independent MgADP phosphorylation reaction. The basic pK observed in both the full forward and reverse reactions suggests that making the active site more negative, through the loss of a proton, results in reduced catalysis for both these reactions.

Interestingly, the partial pH dependence for the phosphorylation reaction, where the dianionic carbamoyl phosphate is a substrate rather than the trianionic carboxyphosphate intermediate in the full reverse reaction, indicates that the active site prefers another negative charge. The wave-shaped k_{cat}/K_m pH profile with carbamoyl phosphate as the variable substrate also indicates that increasing pH facilitates the binding of the non-natural substrate. This could be attributed to the ionization of Glu305 or to some other ionized residue in the active site. Since proton transfer is not involved in the actual catalytic phosphorylation of MgADP, the partial dependence on pH also implies that Glu305 may be protonated in the reverse reaction. Again, while the pKs observed in the pH profiles cannot be unambiguously assigned to specific residues in the BC domain active site, they do appear to agree with the proposed function of Glu305 as the active site base. A comprehensive discussion of the role of the Lys245-Glu305-Glu218 catalytic triad in the wild-type catalyzed pyruvate carboxylation reaction and further implications these pH profiles have on the proposed mechanism is detailed in the accompanying article.[7]

Free Mg^{2+} Lowers the K_a for Acetyl-CoA and Aids in Coupling the Reactions of the BC and CT Domain. The *Re*PC holoenzyme structure[8] revealed the positioning of two Mg^{2+} ions in the BC domain, one which is coordinated to the β- and γ-phosphoryl oxygen of ATP-γ-S and the other which is coordinated to the α- and γ-phosphoryl oxygen. Presumably, one of the Mg^{2+} ions enters the BC domain as the MgATP complex.[24] The initial velocity studies show that MgATP and free Mg^{2+} add to the active site in rapid equilibrium with Mg^{2+} binding first. On the basis of these studies, it is difficult to distinguish between a mechanism where acetyl-CoA initially binds to the enzyme or binds randomly with respect to free Mg^{2+}. Even so, the initial velocity studies indicate that Mg^{2+} binds to the BC domain active site prior to MgATP and HCO_3^-. Since the essential activator binds in the BC domain active site, it was somewhat surprising that increasing concentrations of free Mg^{2+} had marked effects on the initial velocity plots when either acetyl-CoA or pyruvate was the varied component. In both cases, increasing concentrations of free Mg^{2+} increased the k_{cat} for oxaloacetate formation, possibly by aiding in the proper orientation of the γ-phosphate of ATP in the active site. More puzzling is the observed decrease in the K_a for acetyl-CoA (Figure 2). While it could be postulated that Mg^{2+} binding in the BC domain induces significant conformational changes in the allosteric domain which would facilitate the binding of acetyl-CoA and therefore lower the apparent K_a of activation,[24] there is currently no direct structural or kinetic evidence that this occurs in *Re*PC.

The nonlinear dependence of pyruvate on the rate of the oxaloacetate formation at low concentrations of free Mg^{2+} (Figure 1) is indicative of incomplete coupling between the BC and CT domain reactions.[25] Similar concave downward

reciprocal plots have been observed for rat,[26] sheep,[27] and avian PC[28] catalyzed reactions. An investigation of the effects of free Mg^{2+} on the formation and stability of the enzyme−carboxybiotin complex of avian liver PC[20] show that the essential activator significantly decreases the amount of the nonproductive decarboxylation of carboxybiotin in the BC domain and pre-steady-state kinetics[24] confirm that one possible role of Mg^{2+} in the carboxylation reaction is to increase the amount of productive MgATP cleavage.

The Presence of Pyruvate Stimulates the Release of P_i from the BC Domain. The binding of pyruvate in the CT domain, in both the presence and absence of acetyl-CoA, had a significant stimulatory effect on the rate of P_i release from the BC domain. The nearly 300-fold increase in the rate of P_i release observed with subsaturating concentrations of pyruvate could be attributed to either an actual enhancement of the catalytic activity in the BC domain or to promoting the translocation of the BCCP−carboxybiotin domain (Figure 4). The correlation between pyruvate binding and the translocation of the BCCP domain to the CT domain has been well established in kinetic studies with PC.[20,29] While the current study cannot definitively exclude the possibility that pyruvate binding in the CT domain has an effect on the rate of MgATP-hydrolysis and carboxybiotin formation, both structural and kinetic evidence support the idea that the movement of the BCCP−biotin/carboxybiotin domain from the BC domain to the CT domain promotes the release of P_i from the BC domain.

The relative positioning of the BCCP and BC domains, disclosed in the accompanying article,[13] illustrates how the translocation of the BCCP domain upon pyruvate binding would result in the increased rate of P_i release without necessarily increasing the rate of the catalytic reaction. When the BCCP domain is interacting with the BC domain, it is positioned such that the random opening of the B-subdomain is effectively restricted, resulting in the slow release of products. Movement of the BCCP domain to the CT domain upon the binding of pyruvate would result in a significant increase in the rate of P_i release since the B-subdomain lid movements are no longer restricted. Despite the fact that the current crystal structures of the *Re*PC holoenzyme[8,13] give little insight into how pyruvate binding in the CT domain of one polypeptide chain can influence the translocation of the BCCP domain of a neighboring polypeptide chain, the overwhelming kinetic evidence suggests that there is communication between these two active sites mediated through interactions between the BC, CT, and BCCP−biotin domains.

Acetyl-CoA Couples MgATP-Hydrolysis/Carboxybiotin Formation in the BC Domain with Pyruvate Carboxylation in the CT Domain. It is apparent from Table 4, which shows the effect of acetyl-CoA on the specific activities of the various reactions catalyzed by *Re*PC, that reactions involving the formation of the carboxyphosphate intermediate, namely the pyruvate carboxylation, oxaloacetate decarboxylation (full reverse), and HCO_3^--dependent MgATP-cleavage reactions, are most affected by acetyl-CoA. As with the yeast PC isoenzyme 1 (Pyc1), acetyl-CoA had no effect on the rate of MgADP phosphorylation by carbamoyl phosphate,[30] a reaction which does not proceed through the formation of the carboxyphosphate intermediate. Pre-steady-state kinetic studies with avian PC[31] confirm that acetyl-CoA affects the ability of the enzyme to form the carboxyphosphate intermediate.

There are several possible mechanisms by which acetyl-CoA could facilitate the formation of the carboxyphosphate

intermediate, one being to decrease the apparent K_m for HCO_3^-. For example, the apparent K_m for HCO_3^- observed with PC from *B. Thermodenitrificans*[32] was 16 mM in the presence of acetyl-CoA and the absence of acetyl-CoA resulted in a 25-fold increase in the K_m for HCO_3^- (400 mM). Similar effects were observed in *Re*PC where the K_m for HCO_3^- in *Re*PC determined in the presence of acetyl-CoA was 10.8 ± 0.4 mM, comparable to those for other bacterial PCs.[33] A 40-fold decrease in the k_{cat} for oxaloacetate formation was observed when the concentrations of HCO_3^- were decreased from 25 mM (Table 1) to 15 mM (Table 5) in the absence of acetyl-CoA, suggesting that acetyl-CoA may dramatically decrease the apparent K_m for HCO_3^-.

In the presence of acetyl-CoA, a 1:1 coupling between the determined rates of P_i release and oxaloacetate formation is observed at saturating concentrations of pyruvate (Figure 4A). The complete coupling of the reactions of the two domains is not observed until concentrations of pyruvate reach ~1 mM, which is well above the reported intracellular concentrations of pyruvate (0.05−0.15 mM[34]). While inefficient, the abortive nonproductive cleavage of MgATP in the BC domain in the presence of low levels of pyruvate can be explained by previous kinetic isotope effect studies.[35] Once pyruvate binds in the CT domain, stimulating the release of P_i from the BC domain, it is only 50% committed to catalysis and will diffuse out from the active site prior to the arrival of the BCCP−carboxybiotin domain.[35,36] The ability of pyruvate to easily move in and out of the CT domain active site is also reflected in the increased K_m for pyruvate determined for the full forward reaction compared to the K_a for pyruvate determined for the stimulation of P_i release. A definitive metabolic rationale for the observed lack of stoichiometry between the *Re*PC-catalyzed MgATP cleavage in the BC domain and pyruvate carboxylation in the CT domain has not been established, although it is suggestive of a regulatory mechanism where elevated levels of pyruvate cause a hypercompensatory increase in PC efficiency.[37] While energetically inefficient at low concentrations of pyruvate, the amount of coupling between cleavage of MgATP and carboxyl transfer would still allow for the production of an adequate amount of oxaloacetate required to maintain essential anaplerotic and gluconeogenic functions.[11,33,37] Further, given that *Rhizobium etli* contains both phosphoenolpyruvate carboxylase and an α_4 PC, both of which catalyze the MgATP-dependent conversion of pyruvate to oxaloacetate,[11,33] the metabolic consequences of the ineffective use of MgATP at low concentrations of pyruvate by *Re*PC is most likely moderated by complex regulatory and compensatory mechanisms.

The complex, substrate-induced regulation of PC activity and efficiency is intimately intertwined with the allosteric regulation of the enzyme activity by acetyl-CoA. Both the k_{cat} of P_i release and oxaloacetate formation are greatly diminished in the absence of acetyl-CoA, and the reactions of the BC and CT domains are almost completely uncoupled at saturating concentrations of pyruvate. There are several possible reasons for the incomplete coupling of the two domains. If acetyl-CoA has an effect on the positioning and orientation of the CT domain, then its absence may result in pyruvate being tightly bound in the active site or carboxybiotin access to the active site being impeded, resulting in the increased stimulation of P_i release without an accompanying increase in oxaloacetate formation. Acetyl-CoA may also influence the placement of the BCCP domain near the BC domain. If this is true, then in the absence of acetyl-CoA the tethered-biotin may either be improperly positioned or not

inserted into the BC domain, resulting in MgATP-cleavage but no carboxybiotin formation. The structural description of the interactions between the BCCP and BC domains indicate that the BCCP domain plays an active role in closing the B-subdomain lid to create a tighter, more compressed active site.[13] Improper positioning of the BCCP domain could result in the opening of the B-subdomain lid and the release of PO_4^{3-} prior to the deprotonation and carboxylation of the tethered biotin. Not only could the absence of acetyl-CoA result in the premature release of PO_4^{3-}, but a looser active site could also result in the protonation or improper positioning of PO_4^{3-} in the active site.

Kinetic evidence shows that acetyl-CoA is more likely to have an effect on the orientation and positioning of substrates in the BC domain active site. While pre-steady-state kinetic studies with avian PC[24,31] have shown that there is incomplete coupling between MgATP cleavage and carboxybiotin formation in the absence of acetyl-CoA, the current steady-state study cannot differentiate between the rates of P_i release and carboxybiotin formation. In fact, due to the complicated allosteric activation by acetyl-CoA and effects of various substrates on both the conformation and movement of the various domains in *Re*PC, it is conceivable that there are several factors contributing to the uncoupling of the reactions of the two domains in the absence of acetyl-CoA. It is interesting to note that while the stimulatory effect of pyruvate on the release of P_i is not absolutely dependent on acetyl-CoA, it is completely dependent on the presence of tethered biotin,[9] suggesting that the stimulation and, consequently, the communication between the CT and BC domain are mediated through the BCCP−biotin domain.

■ CONCLUSIONS

The current steady-state kinetic study has given valuable insight into the activation and regulation of the α_4 PC from *R. etli*. One of the more interesting aspects of the regulation and coordination of the catalysis in the BC and CT domains is that both activators and substrates will have stimulatory effects on the various reactions in the different active sites. Although the current structural descriptions of the *Re*PC[8,13] and *Sa*PC[14] holoenzymes do not allow for elaboration on the structural basis by which acetyl-CoA and Mg^{2+} couple the MgATP-cleavage/biotin carboxylation in the BC domain with carboxyl transfer in the CT domain, these steady-state kinetic studies do denote a future direction for both kinetic and structural studies.

■ ASSOCIATED CONTENT

Ⓢ Supporting Information

Initial rate vs $\left[HCO_3^-\right]$ plot (Figure S1), initial velocity plots of the rates of pyruvate carboxylation at varied MgATP at fixed Mg^{2+} curves (Figure S2), and the effect of free Mg^{2+} on the rate of MgADP phosphorylation with saturating concentrations of carbamoyl phosphate (Figure S3). This material is available free of charge via the Internet at http://pubs.acs.org.

■ AUTHOR INFORMATION

Corresponding Author
*E-mail: cleland@enzyme.wisc.edu. Phone: (608) 262-1373. Fax: (608) 265-2904.

■ ABBREVIATIONS

PC, pyruvate carboxylase; BC, biotin carboxylase; CT, carboxyl transferase; BCCP, biotin carboxyl carrier protein; ATP, adenosine triphosphate; ADP, adenosine diphosphate; RePC, *Rhizobium etli* PC; hPC, human PC; SaPC, *Staphylococcus aureus* PC; BirA, biotin protein ligase; IPTG, isopropyl-β-D-thiogalactopyranoside; NADH, nicotinamide adenine dinucleotide; acetyl-CoA, acetyl-coenzyme A; NADP⁺, nicotinamide adenine dinucleotide phosphate; Pᵢ, inorganic phosphate; PNP, purine nucleoside phosphorylase; MESG, 2-amino-6-mercapto-7-methylpurine riboside.

■ ADDITIONAL NOTE

[a]All amino acid numbering used in this article is based on the *R. etli* pyruvate carboxylase sequence.

■ REFERENCES

(1) For general reviews of PC function, structure, and mechanism please see: (a) Jitrapakdee, S., Vidal-Puig, A., and Wallace, J. C. (2006) Anaplerotic roles of pyruvate carboxylase in mammalian tissues. *Cell. Mol. Life Sci. 63*, 843−854. (b) Attwood, P. V., and Wallace, J. C. (2002) Chemical and catalytic mechanism of carboxyl transfer reaction in biotin-dependent enzymes. *Acc. Chem. Res. 35*, 113−120. (c) Jitrapakdee, S. St., Maurice, M., Rayment, I, Cleland, W. W., Wallace, J. C., and Attwood, P. V. (2008) Structure, mechanism and regulation of pyruvate carboxylase. *Biochem. J. 413*, 369−387, and the references cited within.

(2) (a) Garcia-Cazorla, A., Rabier, D., Touati, G., Chadefaux-Vekemans, B., Marsac, C., de Lonlay, P., and Saudubray, J.-M. (2006) Pyruvate carboxylase deficiency: metabolic characteristics and new neurological aspects. *Ann. Neurol. 59*, 121−127. (b) Marin-Valencia, I., Roe, C. R., and Pascual, J. M. (2010) Pyruvate carboxylase deficiency: Mechanisms, mimics and anaplerosis. *Mol. Genet. Metab. 101*, 9−17.

(3) Fan, T. W. M., Lane, A. N., Higashi, R. M., Farag, M. A., Gao, H., Bousamra, M., and Miller, D. M. (2009) Altered regulation of metabolic pathways in human lung cancer discerned by ¹³C stable isotope-resolved metabolomics (SIRM). *Mol. Cancer 8*, 1−19.

(4) (a) Jitrapakdee, S., Wutthisathapornchai, A., Wallace, J. C., and MacDonald, M. J. (2010) Regulation of insulin secretion: role of mitochondrial signaling. *Diabetologia 53*, 1019−1032. (b) Jitrapakdee, S., and Wallace, J. C. (1999) Structure, function and regulation of pyruvate carboxylase. *Biochem. J. 340*, 1−16.

(5) (a) Schär, J., Regina Stoll, R., Schauer, K., Loeffler, D. I. M., Eylert, E., Joseph, B., Eisenreich, W., Fuchs, T. M., and Goebel, W. (2010) Pyruvate carboxylase plays a crucial role in carbon metabolism of extra- and intracellularly replicating *Listeria monocytogenes*. *J. Bacteriol. 192*, 1774−1778. (b) Eisenreich, W., Slaghuis, J., Laupitz, R., Bussemer, J., Stritzker, J., Schwarz, C., Schwarz, R., Dandekar, T., Goebel, W., and Bacher, A. (2006) ¹³C isotopologue perturbation studies of *Listeria monocytogenes* carbon metabolism and its modulation by the virulence regulator PrfA. *Proc. Natl. Acad. Sci. U. S. A. 103*, 2040−2045.

(6) (a) Benton, B. M., Zhang, J. P., Bond, S., Pope, C., Christian, T., Lee, L., Winterberg, K. M., Schmid, M. B., and Buysse, J. M. (2004) Large-scale identification of genes required for full virulence of *Staphylococcus aureus*. *J. Bacteriol. 186*, 8478−8489. (b) Kohler, C., Wolff, S., Albrecht, D., Fuchs, S., Becher, D., Büttner, K., Engelmann, S., and Hecker, M. (2005) Proteome analyses of *Staphylococcus aureus* in growing and non-growing cells: a physiological approach. *Int. J. Med. Microbiol. 295*, 547−565.

(7) Zeczycki, T. N., Menefee, A. L., Adina-Zada, A., Jitrapakdee, S., Wallace, J. C., Attwood, P. V., St. Maurice, M., and Cleland, W. W. (2011) Novel Insights into the Biotin Carboxylase Domain Reactions of Pyruvate Carboxylase from *Rhizobium etli*. *Biochemistry*, DOI: dx.doi.org/10.1021/bi2012788.

(8) St. Maurice, M., Reinhardt, L., Surinya, K. H., Attwood, P. V., Wallace, J. C., Cleland, W. W., and Rayment, I. (2007) Domain architecture of pyruvate carboxylase, a biotin-dependent multifunctional enzyme. *Science 317*, 1076−1079.

(9) Zeczycki, T. N. St., Maurice, M., Jitrapakdee, S., Wallace, J. C., Attwood, P. V., and Cleland, W. W. (2009) Insight into the carboxyl transferase domain mechanism of pyruvate carboxylase from *Rhizobium etli*. *Biochemistry 48*, 4305−4313.

(10) Zeczycki, T. N. St., Maurice, M., and Attwood, P. V. (2010) Inhibitors of pyruvate carboxylase. *Open Enzyme Inhib. J. 3*, 8−26.

(11) (a) Encarnacion, S., Dunn, M., Willms, K., and Mora, J. (1995) Fermentative and aerobic metabolism in *Rhizobium etli*. *J. Bacteriol. 177*, 3058−3066. (b) Dunn, M. F., Araicza, G., Cevallos, M. A., and Mora, J. (2006) Regulation of pyruvate carboxylase in *Rhizobium etli*. *FEMS Microbiol. Lett. 157*, 301−306.

(12) Sauer, U., and Eikmanns, B. J. (2005) The PEP-pyruvate-oxaloacetate node as the switch point for carbon flux distribution in bacteria. *FEMS Microbiol. Rev. 29*, 765−794.

(13) Lietzan, A. D., Menefee, A. L., Zeczycki, T. N., Kumar, S., Attwood, P. V., Wallace, J. C., Cleland, W. W. St., and Maurice, M. (2011) Interaction between the biotin carboxyl carrier domain and the biotin carboxylase domain in the asymmetrical pyruvate carboxylase tetramer from *Rhizobium etli*. *Biochemistry*, DOI: dx.doi.org/10.1021/bi201277j.

(14) (a) Xiang, S., and Tong, L. (2008) Crystal structures of huamn and *Staphylococcus aurues* pyruvate carboxylase and molecular insights into the carboxyltransfer reaction. *Nat. Struct. Mol. Biol. 15*, 295−302. (b) Yu, L. P. C., Xiang, S., Lasso, G., Gil, D., Valle, M., and Tong, L. (2009) A Symmetrical Tetramer for *S. aureus* Pyruvate Carboxylase in Complex with Coenzyme A. *Structure 17*, 823−832. (c) Lasso, G., Yu, L. P. C., Gil, D., Xiang, S., Tong, L., and Valle, M. (2010) Cryo-EM Analysis reveals new insights into the mechanism of action of pyruvate carboxylase. *Structure 18*, 1300−1310.

(15) Ellis, K. J., and Morrison, J. F. (1982) Buffers of constant ionic strength for studying pH-dependent processes. *Methods Enzymol. 87*, 405−426.

(16) Cleland, W. W. (1979) Statistical analysis of enzyme kinetic data. *Methods Enzymol. 63*, 103−138.

(17) (a) Cook, P. F. (1982) Kinetic studies to determine the mechanism of bovine liver glutamate dehydrogenase by nucleotide effectors. *Biochemistry 21*, 113−116. (b) Viola, R. E., and Cleland, W. W. (1982) Initial velocity analysis for terreactant mechanisms. *Methods Enzymol. 87*, 353−366.

(18) Adina-Zada, A., Jitrapakdee, S., Surinya, K. H., Mcldowie, M. J., Piggott, M. J., Cleland, W. W., Wallace, J. C., and Attwood, P. V. (2008) Insight into the mechanism and regulation of pyruvate carboxylase by characterization of a biotin-deficient mutant of the *Bacillus thermodenitrificans* enzyme. *Int. J. Biochem. Cell Biol. 40*, 1743−1752.

(19) (a) Keech, D. B., and Utter, M. F. (1963) Pyruvate carboxylase. II. Properties. *J. Biol. Chem. 238*, 2609−2614. (b) Ashman, L. K., Keech, D. B., Wallace, J. C., and Nielsen, J. (1972) Sheep kidney pyruvate carboxylase. Studies on its activation by acetyl coenzyme A and characterization of its acetyl coenzyme A independent reaction. *J. Biol. Chem. 18*, 5818−5824.

(20) (a) Attwood, P. V., Wallace, J. C., and Keech, D. B. (1984) The carboxybiotin complex of pyruvate carboxylase. A kinetic analysis of the effects of Mg²⁺ ions on its stability and on its reaction with pyruvate. *Biochem. J. 219*, 243−251. (b) Attwood, P. V., and Wallace, J. C. (1986) The carboxybiotin complex of chicken liver pyruvate carboxylase. A kinetic analysis of the effects of acetyl-CoA, Mg²⁺ ions and temperature on its stability and on its reaction with 2-oxobutyrate. *Biochem. J. 235*, 359−364.

(21) Attwood, P. V., and Cleland, W. W. (1986) Decarboxylation of oxaloacetate by pyruvate carboxylase. *Biochemistry 25*, 8191−8196.

(22) Ashman, L. K., and Keech, D. B. (1975) Sheep kidney pyruvate carboxylase. Studies on the coupling of adenosine triphosphate hydrolysis and CO_2 fixation. *J. Biol. Chem. 250*, 14−21.

(23) Chou, C.-Y., Yu, L. P. C., and Tong, L. (2009) Crystal structure of biotin carboxylase in complex with substrates and implications for its catalytic mechanism. *J. Biol. Chem. 284*, 11690−11697.

(24) Branson, J. P., and Attwood, P. V. (2000) Effects of Mg^{2+} on the pre-steady-state kinetics of the biotin carboxylation reaction of pyruvate carboxylase. *Biochemistry 39*, 7480−7491.

(25) Easterbrook-Smith, S. B., Wallace, J. C., and Keech, D. B. (1978) A reappraisal of the reaction pathway of pyruvate carboxylase. *Biochem. J. 169*, 225−228.

(26) McClure, W. R., Lardy, H. A., and Kneifel, H. P. (1971) Rate liver pyruvate carboxylase I. Preparation, properties and cation specificity. *J. Biol. Chem. 246*, 3569−3578.

(27) Scrutton, M. C., Keech, D. B., and Utter, M. F. (1965) Pyruvate carboxylase IV. Partial reactions and the locus of activation by acetyl coenzyme A. *J. Biol. Chem. 240*, 574−581.

(28) Taylor, H., Nielsen, J., and Keech, D. B. (1969) Substrate activation of pyruvate carboxylase by pyruvate. *Biochem. Biophys. Res. Commun. 37*, 723−728.

(29) Goodall, G. J., Baldwin, G. S., Wallace, J. C., and Keech, D. B. (1981) Factors that influence the translocation of the N-carboxybiotin moiety between the two sub-sites of pyruvate carboxylase. *Biochem. J. 199*, 603−609.

(30) (a) Branson, J. P., Nezic, M., Wallace, J. C., and Attwood, P. V. (2002) Kinetic characterization of yeast pyruvate carboxylase isozyme Pyc1. *Biochemistry 41*, 4459−4466. (b) Branson, J. P., Nezic, M., Jitrapakdee, S., Wallace, J. C., and Attwood, P. V. (2004) Kinetic characterization of yeast pyruvate carboxylase isozyme Pyc1 and the Pyc1 mutant, C249A. *Biochemistry 43*, 1075−1081.

(31) Legge, G. B., Branson, J. P., and Attwood, P. V. (1996) Effects of acetyl CoA on the pre-steady-state kinetics of the biotin carboxylation reaction of pyruvate carboxylase. *Biochemistry 35*, 3849−3856.

(32) Libor, S. M., Sundaram, T. K., and Scrutton, M. C. (1978) Pyruvate carboxylase from a thermophilic *Bacillus*. Studies on the specificity of activation by acyl derivatives of coenzyme A and on the properties of catalysis in the absence of activator. *Biochem. J. 169*, 543−558.

(33) (a) Dunn, M. F., Encarnación, S., Araíza, G., Vargas, M. C., Dávalos, A., Peralta, H., Mora, Y., and Mora, J. (1996) Pyruvate carboxylase from *Rhizobium etli*: mutant characterization, nucleotide sequence, and physiological role. *J. Bacteriol. 178*, 5960−5970. (b) Dunn, M. F., Araíza, G., and Finan, T. M. (2001) Cloning and characterization of the pyruvate carboxylase from *Sniorhizobium meliloti* Rm1021. *Arch. Microbiol. 176*, 355−363.

(34) Williamson, D. H., and Brosnan, J. T. (1974) Concentrations of metabolites in animal tissues. In *Methods of Enzymatic Analysis*, 2nd ed. (Bergmeyer, H. U., Ed.) Vol. 4, pp 2266−2302, Academic Press, New York.

(35) Cheung, Y.-F., and Walsh, C. (1976) Studies on the intramolecular and intermolecular kinetic isotope effects in pyruvate carboxylase catalysis. *Biochemistry 15*, 3749−3754.

(36) Warren, G. B., and Tipton, K. F. (1974) Pig liver pyruvate carboxylase. The reaction pathway for the carboxylation of pyruvate. *Biochem. J. 139*, 311−320.

(37) Easterbrook-Smith, S. B., Hudson, P. J., Goss, N. H., Keech, D. B., and Wallace, J. C. (1976) Pyruvate carboxylase: Mechanism of the second partial reaction. *Arch. Biochem. Biophys. 176*, 709−720.